Microcanonical finite-size scaling in second-order phase transitions with diverging specific heat

L. A. Fernandez,[1,2] A. Gordillo-Guerrero,[3,2] V. Martin-Mayor,[1,2] and J. J. Ruiz-Lorenzo[4,2]
[1]*Departamento de Física Teórica I, Universidad Complutense, 28040 Madrid, Spain*
[2]*Instituto de Biocomputación and Física de Sistemas Complejos (BIFI), 50009 Zaragoza, Spain*
[3]*Departamento de Ingeniería Eléctrica, Electrónica y Automática, Universidad de Extremadura, 10071 Caceres, Spain*
[4]*Departamento de Física, Universidad de Extremadura, 06071 Badajoz, Spain*
(Received 28 May 2009; revised manuscript received 23 September 2009; published 6 November 2009)

A microcanonical finite-size ansatz in terms of quantities measurable in a finite lattice allows extending phenomenological renormalization (the so-called quotients method) to the microcanonical ensemble. The ansatz is tested numerically in two models where the canonical specific heat diverges at criticality, thus implying Fisher renormalization of the critical exponents: the three-dimensional ferromagnetic Ising model and the two-dimensional four-state Potts model (where large logarithmic corrections are known to occur in the canonical ensemble). A recently proposed microcanonical cluster method allows simulating systems as large as $L=1024$ (Potts) or $L=128$ (Ising). The quotients method provides accurate determinations of the anomalous dimension, η, and of the (Fisher-renormalized) thermal ν exponent. While in the Ising model the numerical agreement with our theoretical expectations is very good, in the Potts case, we need to carefully incorporate logarithmic corrections to the microcanonical ansatz in order to rationalize our data.

DOI: 10.1103/PhysRevE.80.051105 PACS number(s): 05.50.+q, 64.60.Cn, 75.40.Mg

I. INTRODUCTION

The canonical ensemble enjoys a predominant position in theoretical physics due to its many technical advantages (convex effective potential on finite systems, easily derived fluctuation-dissipation theorems, etc.) [1]. This somehow arbitrary choice of ensemble is justified by the ensemble equivalence property that holds in the thermodynamic limit for systems with short-range interactions.

However, in spite of this long-standing prejudice in favor of the canonical ensemble, the canonical analysis of phase transitions is *not* simpler. The advantages of microcanonical analysis of first-order phase transitions has long been known [2,3] and indeed become overwhelming in the study of disordered systems [4]. Furthermore, the current interest in mesoscopic or even nanoscopic systems, where ensemble equivalence does not hold, provides ample motivation to study other statistical ensembles and, in particular, the microcanonical one [5]. Besides, microcanonical Monte Carlo [6] is now as simple and efficient as its canonical counterpart (even microcanonical cluster algorithms are known [3]). Under such circumstances, it is of interest the extension to the microcanonical framework of finite-size scaling (FSS) [7–10] for systems undergoing a continuous phase transition.

The relation between the microcanonical and the canonical critical behaviors is well understood only in the thermodynamic limit. A global constraint modifies the critical exponents, but only if the specific heat of the unconstrained system diverges with a positive critical exponent $\alpha>0$ [11] (however, see [12]). The modification in the critical exponents, named Fisher renormalization, is very simple. Let L be the system size and consider an observable O (for instance, the susceptibility) whose diverging behavior in the infinite-volume canonical system is governed by the critical exponent x_O [13]

$$\langle O\rangle^{\text{canonical}}_{L=\infty,T} \propto |t|^{-x_O}, \quad t=\frac{T-T_c}{T_c}. \tag{1}$$

Now, let e be the internal energy density and $e_c=\langle e\rangle^{\text{canonical}}_{L=\infty,T_c}$. Consider the microcanonical expectation value of the *same* observable O in Eq. (1), but now at fixed energy e. The scaling behavior (1) translates to [14]

$$\langle O\rangle_{L=\infty,e} \propto |e-e_c|^{-x_{O,m}}, \quad x_{O,m}=\frac{x_O}{1-\alpha}. \tag{2}$$

We will denote the microcanonical exponents with the subindex "m." Hence, the Fisher renormalization of the correlation length, ξ, exponent $x_\xi=\nu$, is $\nu\to\nu_m=\nu/(1-\alpha)$, that of the order parameter, M, exponent is $x_M=\beta\to\beta_m=\beta/(1-\alpha)$, etc. On the other hand, the anomalous dimension, defined in Eq. (26), is invariant under Fisher renormalization [11], i.e. $\eta=\eta_m$ (see also [15] for a recent extension of Fisher renormalization to the case of *logarithmic* scaling corrections).

As for systems of finite size, the microcanonical FSS [16–18] is at the level of an ansatz, which is obtained from the canonical one merely by replacing the free-energy density by the entropy density and using Fisher-renormalized critical exponents. The microcanonical ansatz reproduces the canonical one [19] and it has been subject of some numerical testings [18,20]. Furthermore, systems undergoing Fisher renormalization (due to a global constraint other than the energy) do seem to obey FSS as well [21].

A difficulty lies in the fact that the current forms of the microcanonical FSS ansatz (FSSA) [16–18] are in a somehow old-fashioned form. Indeed, they are formulated in terms of quantities such as e_c or the critical exponents, which are not accessible in the absence of an analytical solution. In this respect, a progress was achieved in a canonical context [22] when it was realized that the finite-lattice correlation length [23] allows to formulate the FSSA in terms of quantities computable in a finite lattice. This formulation made

practical to extend Nightingale's phenomenological renormalization [24] to space dimensions $D>2$ (the so-called quotients method [25]).

Here, we will extend the microcanonical FSSA to a modern form, allowing us to use the quotients method. We will test numerically this extended FSSA in two models with $\alpha>0$, hence undergoing nontrivial Fisher renormalization, namely, the $D=3$ ferromagnetic Ising model and the $D=2$ four-state ferromagnetic Potts model. The Potts model has the added interest of exhibiting, in its canonical form, quite strong *logarithmic* corrections to scaling that are nevertheless under relatively strong analytical control (see [26–30]). It will be, therefore, quite a challenge to control the logarithmic corrections within the microcanonical setting.

The layout of the rest of this paper is as follows. In Sec. II, we briefly recall the particular microcanonical ensemble used in this work (Lustig's microcanonical setup [6], where the fluctuation-dissipation formalism of [3] applies). In Sec. III, we present our extended microcanonical FSSA. A brief description of simulated models and measured observables is presented in Sec. IV while the specific simulation details are given in Sec. V. The results both for the $D=3$ Ising model and for the $D=2$ Potts model are given in Secs. VI and VII, respectively. Finally, we devote Sec. VIII to the conclusions. In addition, in the Appendix, we propose an extension of the quotients method, aimed to speed up convergence to the large L limit in the presence of multiplicative logarithmic corrections.

II. MICROCANONICAL ENSEMBLE

The first step in the construction of the ensemble is an extension of the configuration space. We add $N(=L^D)$ real momenta, p_i, to our N original variables, σ_i (named spins here) [3,6]. Note that this extended configuration, $\{\sigma_i,p_i\}$, appears in many numerical schemes (consider, for instance, hybrid Monte Carlo [31] simulations in lattice gauge theory). We shall work in the *microcanonical* ensemble for the $\{\sigma_i,p_i\}$ system.

Let $\mathcal{U}$ be the original spin Hamiltonian [e.g., Eq. (36) in our case]. Our total energy is [32]

$$\mathcal{E}=\sum_{i=1}^{N}\frac{p_i^2}{2}+\mathcal{U}\quad(e\equiv\mathcal{E}/N,u\equiv\mathcal{U}/N). \tag{3}$$

The momenta contribution,

$$N\kappa\equiv\sum_{i=1}^{N}\frac{p_i^2}{2}, \tag{4}$$

is necessarily positive and it is best thought of as a "kinetic" energy. In this mechanical analog, the original spin Hamiltonian $\mathcal{U}$ can be regarded as a "potential" energy.

The canonical partition function is ($\beta\equiv1/T$),

$$Z_N(\beta)=\int_{-\infty}^{\infty}\prod_{i=1}^{N}dp_i\sum_{\{\sigma_i\}}\mathrm{e}^{-\beta\mathcal{E}}=\left(\frac{2\pi}{\beta}\right)^{N/2}\sum_{\{\sigma_i\}}e^{-\beta\mathcal{U}}, \tag{5}$$

where $\Sigma_{\{\sigma_i\}}$ denotes summation over spin configurations. Hence, the $\{p_i\}$ play the role of a Gaussian thermostat. The $\{p_i\}$ are statistically uncorrelated with the spins. Since $\langle\kappa\rangle_{L,\beta}^{\text{canonical}}=1/(2\beta)$, one has $\langle e\rangle_\beta^{\text{canonical}}=\langle u\rangle_\beta^{\text{canonical}}+1/(2\beta)$.

Furthermore, given the statistical independence of κ and u, the canonical probability distribution function for e, $P_\beta^{(L)}(e)$, is merely the convolution of the distributions for κ and u,

$$P_\beta^{(L)}(e)=\int_0^\infty d\kappa P_\beta^{(L),\kappa}(\kappa)P_\beta^{(L),u}(e-\kappa). \tag{6}$$

In particular, note that for spin systems on a finite lattice, $P_\beta^{(L),u}(u)$ is a sum of (order N) Dirac's δ functions. Now, since the canonical variance of κ is $1/(\beta\sqrt{2N})$, roughly $\sqrt{N}$ discrete u levels, with $u\sim e-1/(2\beta)$, give the most significant contribution to $P_\beta^{(L)}(e)$. We see that the momenta's kinetic energy provide a natural smoothing of the comblike $P_\beta^{(L),u}(u)$. Once we have a conveniently smoothed $P_\beta^{(L)}(e)$, we may proceed to the definition of the entropy.

In a microcanonical setting, the crucial role is played by the entropy density, $s(e,N)$, given by

$$\exp[Ns(e,N)]=\int_{-\infty}^{\infty}\prod_{i=1}^{N}dp_i\sum_{\{\sigma_i\}}\delta(Ne-\mathcal{E}). \tag{7}$$

Integrating out the $\{p_i\}$ using Dirac's delta function in Eq. (7), we get

$$\exp[Ns(e,N)]=\frac{(2\pi N)^{N/2}}{N\Gamma(N/2)}\sum_{\{\sigma_i\}}\omega(e,u,N), \tag{8}$$

$$\omega(e,u,N)\equiv(e-u)^{N/2-1}\theta(e-u). \tag{9}$$

The step function, $\theta(e-u)$, enforces $e>u$. Equation (8) suggests to define the microcanonical average at fixed e of any function of e and the spins, $O(e,\{\sigma_i\})$, as [6]

$$\langle O\rangle_e\equiv\frac{\sum_{\{\sigma_i\}}O(e,\{\sigma_i\})\omega(e,u,N)}{\sum_{\{\sigma_i\}}\omega(e,u,N)}. \tag{10}$$

We use Eq. (8) to compute ds/de [3]:

$$\frac{ds(e,N)}{de}=\langle\hat{\beta}(e;\{\sigma_i\})\rangle_e, \tag{11}$$

$$\hat{\beta}(e;\{\sigma_i\})\equiv\frac{N-2}{2N(e-u)}. \tag{12}$$

Keeping in mind the crucial role of the generating functional in field theory (see, e.g., [10]), we extend the definition (7) by considering a linear coupling between the spins and a site-dependent source field h_i,

$$\exp[Ns(e,\{h_i\},N)]=\int_{-\infty}^{\infty}\prod_{i=1}^{N}dp_i\sum_{\{\sigma_i\}}\exp\left(\sum_i h_i\sigma_i\right)\delta(Ne-\mathcal{E}), \tag{13}$$

where $\mathcal{E}=Ne$ is still given by Eq. (3) without including the source term. In this way, the microcanonical spin-correlation

functions follow from derivatives of $s(e,\{h_i\},N)$,

$$\left.\frac{\partial[Ns]}{\partial h_k}\right|_{e,\{h_i\},N} = \langle\sigma_k\rangle_{e,\{h_i\}},$$

$$\left.\frac{\partial^2[Ns]}{\partial h_k\,\partial h_l}\right|_{e,\{h_i\},N} = \langle\sigma_k\sigma_l\rangle_{e,\{h_i\}} - \langle\sigma_k\rangle_{e,\{h_i\}}\langle\sigma_l\rangle_{e,\{h_i\}}. \quad (14)$$

In particular, if the source term is uniform $h_i=h$, we observe that the microcanonical susceptibility is given by standard fluctuation-dissipation relations [see Ref. [10] and Eq. (43) below].

A. Ensemble equivalence

Equation (7) ensures that the *canonical* probability density function for e is

$$P_\beta^{(L)}(e) = \frac{N}{Z_N(\beta)}\exp\{N[s(e,N)-\beta e]\}, \quad (15)$$

hence, Eq. (11),

$$\log P_\beta^{(L)}(e_2) - \log P_\beta^{(L)}(e_1) = N\int_{e_1}^{e_2} de(\langle\hat{\beta}\rangle_e - \beta), \quad (16)$$

being log() the natural logarithm everywhere in the paper.

The relation between the canonical and the microcanonical spin values is given by

$$\langle O\rangle_\beta^{\text{canonical}} = \int_{-\infty}^{\infty} de\langle O\rangle_e P_\beta^{(L)}(e). \quad (17)$$

Now, Eqs. (15) and (17) imply that the canonical mean value will be dominated by a saddle point at e^{SP},

$$\langle\hat{\beta}\rangle_{e_{L,\beta}^{\text{SP}}} = \beta, \quad (18)$$

which can be read as yet another expression of thermodynamics' second law, $Tds=de$.

The condition of thermodynamic stability (namely, that $\langle\hat{\beta}\rangle_e$ be a monotonically decreasing function of e) ensures that the saddle point is unique and that e^{SP} is a maximum of $P_\beta(e)$. Under the thermodynamic stability condition and if, in the large L limit,

$$\left.\frac{d\langle\hat{\beta}\rangle_e}{de}\right|_{e_{L,\beta}^{\text{SP}}} < 0, \quad (19)$$

the saddle-point approximation becomes exact,

$$e_{L=\infty,\beta}^{\text{SP}} = \langle e\rangle_{L=\infty,\beta}^{\text{canonical}}, \quad (20)$$

and we have ensemble equivalence

$$\langle O\rangle_{L=\infty,e_{L=\infty,\beta}^{\text{SP}}} = \langle O\rangle_{L=\infty,\beta}^{\text{canonical}}. \quad (21)$$

It follows that the microcanonical estimator

$$C_m(L,e) = \frac{1}{d\langle\hat{\beta}\rangle_{e,L}/de}, \quad (22)$$

evaluated at $e_{L=\infty,\beta}^{\text{SP}}$ will tend in the large-L limit to minus the canonical specific heat. Thus, if the critical exponent α is positive, Eq. (19) will fail precisely at e_c. Hence, Eq. (21) can be expected to hold for all e but e_c (or for all β but β_c).

B. Double peaked histogram

The situation can be slightly more complicated if $P_{\beta_c}(e)$ presented two local maxima, remindful of phase coexistence. This is actually the case for one of our models, the $D=2$, four-state Potts model [33]. From Eq. (16), it is clear that the solution to the saddle-point equation (18) will no longer be unique. We borrow the following definitions from the analysis of first-order phase transitions (where true phase coexistence takes place) [3]:

(i) The rightmost root of Eq. (18), $e_{L,\beta}^d$, is a local maximum of $P_\beta^{(L)}$ corresponding to the "disordered phase."

(ii) The leftmost root of Eq. (18), $e_{L,\beta}^o$, is a local maximum of $P_\beta^{(L)}$ corresponding to the "ordered phase."

(iii) The second rightmost root of Eq. (18), $e_{L,\beta}^*$, is a local minimum of $P_\beta^{(L)}$.

Maxwell's construction yields the finite-system critical point, $\beta_{c,L}$ (see Fig. 9),

$$0 = \int_{e_{L,\beta_{c,L}}^o}^{e_{L,\beta_{c,L}}^d} de(\langle\hat{\beta}\rangle_e - \beta_{c,L}), \quad (23)$$

and the finite-system estimator of the "surface tension"

$$\Sigma^L = \frac{N}{2L^{D-1}}\int_{e_{L,\beta_{c,L}}^*}^{e_{L,\beta_{c,L}}^d} de(\langle\hat{\beta}\rangle_e - \beta_{c,L}). \quad (24)$$

Of course, in the large-L limit and for a continuous transition $\Sigma^L\to 0$, $\beta_c^L\to\beta_c$, and $e_{L,\beta_{c,L}}^d, e_{L,\beta_{c,L}}^o \to e_c$.

III. OUR MICROCANONICAL FINITE-SIZE SCALING ANSATZ

Usually, the microcanonical FSSA takes the form of a scaling form for the entropy density [16–18]. In close analogy with the canonical case, one assumes that $s(e,\{h_{\vec{x}}\},N)$ can be divided in a regular part and a singular term $s_{\text{sing}}(e,\{h_{\vec{x}}\},N)$. The regular part is supposed to converge for large L (recall that $N=L^D$) to a smooth function of its arguments. Hence, all critical behavior comes from $s_{\text{sing}}(e,\{h_{\vec{x}}\},N)$. Note as well that we write $\{h_{\vec{x}}\}$, instead of $\{h_i\}$, to emphasize the spatial dependence of the sources (supposedly very mild [10]). Hence,

$$s_{\text{sing}}(e,\{h_{\vec{x}}\},N) = L^{-D}g(L^{1/\nu_m}|e-e_c|,\{L^{y_h}h_{\vec{x}}\}). \quad (25)$$

Here, g is a very smooth function of its arguments, while $y_h=1+\frac{D-\eta}{2}$ is the canonical exponent (see e.g., [10]) which does not get Fisher-renormalized. Corrections to FSS due to irrelevant scaling fields have not played a major role in several previous analysis [16–18] (in [18], only analytical scaling corrections were considered), but will be important for our precision tests. Leading-order corrections were, however, explicitly considered in Ref. [21]. We will propose here alternative forms of the ansatz (25) more suitable for a numerical work where neither e_c nor the critical exponents are known beforehand.

Our first building block is the infinite-system microcanonical correlation length, $\xi_{\infty,e}$. Indeed, ensemble equivalence implies that, in an infinite system, the long-distance behavior of the microcanonical spin-spin propagator $G(\vec{r};e)=\langle\sigma_{\vec{x}}\sigma_{\vec{x}+\vec{r}}\rangle_e-\langle\sigma_{\vec{x}}\rangle_e\langle\sigma_{\vec{x}+\vec{r}}\rangle_e$ behaves for large $\vec{r}$ as in the canonical ensemble (close to a critical point $\xi_{\infty,e}$ is large, so that rotational invariance is recovered in our lattice systems)

$$G(\vec{r};e)=\frac{A}{r^{D-2+\eta}}e^{-r/\xi_{\infty,e}}, \tag{26}$$

where A is a constant. In particular, note that ensemble equivalence implies that the anomalous dimension η does not get Fisher-renormalized. We expect $\xi_{\infty,e}=\xi_{\infty,T}^{\text{canonical}}$ if the correspondence between e and T is fixed through $e=\langle e\rangle_{L=\infty,T}^{\text{canonical}}$.

The basic assumption underlying the FSSA is that the approach to the $L\to\infty$ limit is governed by the dimensionless ratio $L/\xi_{\infty,e}$. Hence, our first form of the microcanonical FSSA for the observable O whose critical behavior was discussed in Eq. (2) is

$$\langle O\rangle_{L,e}=L^{x_{O,m}/\nu_m}f_O(L/\xi_{\infty,e})+\cdots. \tag{27}$$

In the above, the dots stand for scaling corrections, while the function f_O is expected to be very smooth (i.e. differentiable to a large degree or even analytical). A second form of the microcanonical FSSA is obtained by substituting the scaling behavior $\xi_{\infty,e}\propto|e-e_c|^{-\nu_m}$,

$$\langle O\rangle_{L,e}=L^{x_{O,m}/\nu_m}\tilde{f}_O(L^{1/\nu_m}|e-e_c|)+\cdots. \tag{28}$$

Again, $\tilde{f}_O$ is expected to be an extremely smooth function of its argument [34]. In particular, this is the form of the ansatz that follows from Eq. (25) by differentiating with respect to e or from the source terms.

However, the most useful form of the microcanonical FSSA is obtained by applying Eq. (27) to the finite-lattice correlation length $\xi_{L,e}$, obtained in a standard way (see Ref. [10]) from the finite-lattice microcanonical propagator. We expect $\xi_{L,e}/L$ to be a smooth, one-to-one function of $L/\xi_{\infty,e}$, that can be inverted to yield $L/\xi_{\infty,e}$ as a function of $\xi_{L,e}/L$. Hence, our preferred form of the FSSA is

$$\langle O\rangle_{L,e}=L^{x_{O,m}/\nu_m}\left[F_O\left(\frac{\xi_{L,e}}{L}\right)+L^{-\omega}G_O\left(\frac{\xi_{L,e}}{L}\right)+\cdots\right]. \tag{29}$$

Here, F_O and G_O are smooth functions of their arguments and ω is the first universal scaling corrections exponent.

It is important to note that exponent ω does not get Fisher-renormalized. Indeed, let us consider an observable O with critical exponent x_O at a temperature T such that $e=\langle e\rangle_{L=\infty,T}^{\text{canonical}}$. Now, ensemble equivalence tells us that $O_{L=\infty,T}^{\text{canonical}}=O_{L=\infty,e}$ and that $\xi_{L=\infty,T}^{\text{canonical}}=\xi_{L=\infty,e}$. Eliminating T in favor of $\xi_{L=\infty,T}^{\text{canonical}}$ (see, e.g., [10]), we have

$$O_{L=\infty,T}^{\text{canonical}}=\xi_{L=\infty,e}^{x_O/\nu}[A_0+B_O\xi_{L=\infty,e}^{-\omega}+\cdots], \tag{30}$$

where A_0 and B_0 are scaling amplitudes. It follows that $\omega_m=\omega$ and that $x_O/\nu=x_{O,m}/\nu_m$.

Quotients method

Once we have Eq. (29) in our hands, it is straightforward to generalize the quotients method [25]. In the Appendix, we describe how it should be modified in the presence of (multiplicative) logarithmic corrections to scaling.

Let us compare data obtained *at the same* value of e for a pair of lattices $L_1=L$ and $L_2=sL$ with $s>1$. We expect that a single e_{c,L_1,L_2} exists such that the correlation length in units of the lattice size coincides for both systems

$$\frac{\xi_{L,e_{c,L_1,L_2}}}{L}=\frac{\xi_{sL,e_{c,L_1,L_2}}}{sL}. \tag{31}$$

Hence, if we compare now in the two lattices the observable O in Eq. (29), precisely at $e_{c,L,sL}$, we have

$$\frac{\langle O\rangle_{sL,e_{c,L_1,L_2}}}{\langle O\rangle_{L,e_{c,L_1,L_2}}}=s^{x_{O,m}/\nu_m}[1+A_{O,s}L^{-\omega}+\cdots], \tag{32}$$

where $A_{O,s}$ is a nonuniversal scaling amplitude. One considers this equation for fixed s (typically $s=2$) and uses it to extrapolate to $L=\infty$ the L-dependent estimate of the critical exponents ratio $x_{O,m}/\nu_m$. At the purely numerical level, mind as well that there are strong statistical correlations between the quotients in Eqs. (31) and (32) that reduces the statistical errors in the estimate of critical exponents. These errors can be computed via a jackknife method (see, e.g., [10]).

In this work, we shall compute the critical exponents from the following operators (χ is the susceptibility, while ξ is the correlation length, see Sec. IV for definitions):

$$\chi\to x_O=\nu_m(2-\eta), \tag{33}$$

$$\partial_e\xi\to x_O=\nu_m+1. \tag{34}$$

As for the L dependence of $e_{c,L,sL}$, it follows from Eq. (28) as applied to ξ_L/L for the two lattice sizes L and sL [7,10]

$$e_{c,L,s}=e_c+B\frac{1-s^{-\omega}}{s^{1/\nu_m}-1}L^{-(\omega+1/\nu_m)}+\cdots \tag{35}$$

(B is again a nonuniversal scaling amplitude). In particular, if one works at fixed s, $e_{c,L,sL}$ tends to e_c for large L as $L^{-(\omega+1/\nu_m)}$ [35].

IV. MODELS AND OBSERVABLES

We will define here the Hamiltonian and observables of a generic D-dimensional Q-states Potts model. The numerical study has been done for two instances of this model: the three-dimensional Ising ($Q=2$) model and the two-dimensional $Q=4$ Potts model.

We place the spins $\sigma_i=1,\ldots,Q$ at the nodes of a hypercubic D-dimensional lattice with linear size L and periodic boundary conditions. The Hamiltonian is

$$\mathcal{U} = -\sum_{\langle i,j \rangle} \delta_{\sigma_i \sigma_j}, \tag{36}$$

where $\langle i,j \rangle$ denotes first nearest neighbors. For a given spin, σ, we define the normalized Q-vector $\vec{s}$, whose qth component is

$$s_q = \sqrt{\frac{Q}{Q-1}} \left(\delta_{\sigma q} - \frac{1}{Q} \right). \tag{37}$$

A Q components order parameter for the ferromagnetic transition is

$$\vec{\mathcal{M}} = \frac{1}{L^D} \sum_i \vec{s}_i, \tag{38}$$

where i runs over all the lattice sites. We will now consider microcanonical averages. The spatial correlation function is

$$C(\boldsymbol{r}' - \boldsymbol{r}) = \langle \vec{s}(\boldsymbol{r}) \cdot \vec{s}(\boldsymbol{r}') \rangle_e = \frac{Q}{Q-1} \left\langle \delta_{\sigma(\boldsymbol{r})\sigma(\boldsymbol{r}')} - \frac{1}{Q} \right\rangle_e. \tag{39}$$

Our definition for the correlation length at a given internal energy density e is computed from the Fourier transform of C,

$$\hat{C}(\boldsymbol{k}) = \sum_{\boldsymbol{r}} C(\boldsymbol{r}) e^{i\boldsymbol{k}\cdot\boldsymbol{r}}, \tag{40}$$

at zero and minimal ($\|\boldsymbol{k}_{\min}\| = 2\pi/L$) momentum [10,23]

$$\xi(e,L) = \frac{\sqrt{\hat{C}(0)/\hat{C}(\boldsymbol{k}_{\min}) - 1}}{2 \sin(\pi/L)}. \tag{41}$$

Note that $\hat{C}$ can be easily computed in terms of the Fourier transform of the spin field, $\hat{s}(\boldsymbol{k})$, as

$$\hat{C}(\boldsymbol{k}) = L^D \langle \hat{s}(\boldsymbol{k}) \cdot \hat{s}(-\boldsymbol{k}) \rangle_e \tag{42}$$

and that the microcanonical magnetic susceptibility is

$$\chi = L^D \langle \vec{\mathcal{M}}^2 \rangle_e = \hat{C}(0). \tag{43}$$

For the specific case of the Ising model, the traditional definitions, using $S_i = \pm 1$ (recall that $s_i = \pm 1/\sqrt{2}$), are related with those of the general model through

$$\mathcal{U}^{\text{Ising}} = -\sum_{\langle i,j \rangle} S_i S_j = 2\mathcal{U} - 3L^D,$$

$$\beta^{\text{Ising}} = \beta/2,$$

$$\chi^{\text{Ising}} = 2\chi. \tag{44}$$

Notice that in $D=2$, this model undergoes a phase transition in $\beta_c = \log(1+\sqrt{Q})$ which is second order for $Q \leq 4$ and first order for $Q > 4$ [36].

V. SIMULATION DETAILS

We have simulated systems of several sizes in a suitable range of energies (see Table I). To update the spins, we used a Swendsen-Wang (SW) version of the microcanonical cluster method [3]. This algorithm depends on a tunable parameter, κ, which should be as close as possible to $\langle \hat{\beta} \rangle_e$ in order to maximize the acceptance of the SW attempt (SWA). This requires a start up using a much slower METROPOLIS algorithm for determining κ. In practice, we performed cycles consisting of 2×10^3 METROPOLIS steps, κ refreshing, 2×10^3 SWA, and a new κ refreshing. We require an acceptance exceeding 60% to finish these prethermalization cycles fixing κ for the following main simulation where only the cluster method is used.

In both studied cases, we have observed a very small autocorrelation time for all energy values at every lattice size. In the largest lattice for the four states Potts model, we have also consider different starting configurations: hot, cold, and mixed (strips). Although the autocorrelation time is much smaller, for safety, we decided to discard the first 10% of the Monte Carlo history using the last 90% for taking measurements.

TABLE I. Simulation details for the two considered models. For each lattice size L, we show the number of measurements N_m at each energy and the total number of simulated energies uniformly distributed in the displayed energy range N_e. For the $Q=4$, $D=2$ model, the value of N_m reported have been reached only at specific energies near the peaks of the Maxwell's construction. Also, additional nonuniformly distributed energy values have been simulated near the peaks.

Model	L	N_m ($\times 10^6$)	N_e	Energy range
$Q=2$, $D=3$	8	20	42	[−0.8, −0.9]
	12	20	42	[−0.8, −0.9]
	16	20	49	[−0.8, −0.9]
	24	20	25	[−0.845, −0.875]
	32	20	16	[−0.87, −0.860625]
	48	20	10	[−0.87, −0.860625]
	64	5	10	[−0.870625, −0.865]
	96	5	10	[−0.870625, −0.865]
	128	5	7	[−0.869375, −0.865625]
$Q=4$, $D=2$	32	1024	61	[−1.2, −0.9]
	64	128	61	[−1.2, −0.9]
	128	32	41	[−1.08, −0.98]
	256	32	24	[−1.08, −1.005]
	512	25.6	32	[−1.07, −1.01]
	1024	6.4	30	[−1.06, −1.02]

VI. RESULTS FOR THE $D=3$ ISING MODEL

In Fig. 1 (upper panel), we show a scaling plot of the correlation length (in lattice size units) against $(e-e_c)L^{1/\nu_m}$. For the susceptibility, we plot $\chi \sim L^{2-\eta}$ (lower panel). If data followed the expected asymptotic critical behavior with microcanonical critical exponents, they should collapse in a single curve. In Fig. 1, we have used the canonical critical quantities from Refs. [37,38] transformed to the microcanonical counterparts using Eq. (2). From the plot, it is clear

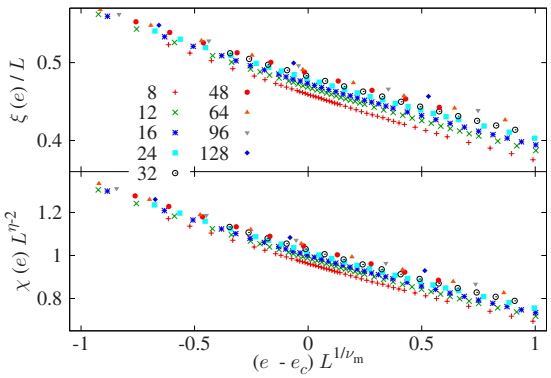

FIG. 1. (Color online) Scaling plot of the correlation length (in lattice size units) and the scaled susceptibility for the three-dimensional Ising model. We used the critical values $e_c = -0.867\,433$ and $\nu_m = 0.7077$. Notice the strong scaling corrections for the small systems, as well as the data collapse for the largest lattices.

that important scaling corrections exist in both cases for the smallest lattices although they are mainly eliminated in the biggest systems.

To obtain the microcanonical critical exponents, we used the quotients method (see Sec. III). The clear crossing points of the correlation length for different lattice sizes can be seen in Fig. 2. The determination of the different quantities at the crossings, and the position of the crossing itself, requires to interpolate the data between consecutive simulated energies. We have found that the method of choice, given the high number of energy values available, is to fit, using the least-squares method, a selected number of points near the crossing to a polynomial of appropriate degree. Straight lines do not provide good-enough fits, however, second- and third-order polynomials give compatible results. In practice, we have fitted a second-order polynomial using the nine nearest points to the crossing, also comparing the results to those using the seven nearest points that turn out fully compatible. For error determination, we have always used a jackknife procedure.

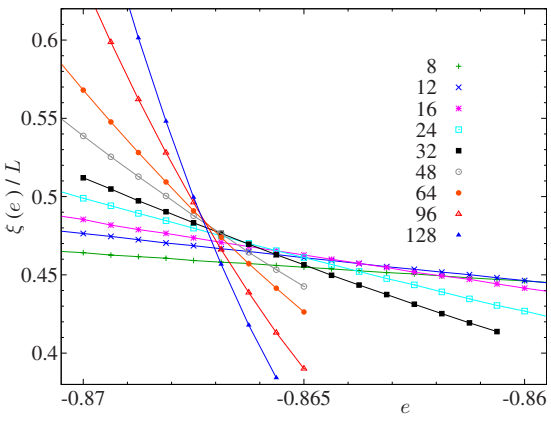

FIG. 2. (Color online) Crossing points of the correlation length in lattice size units for the three-dimensional Ising model. The error bars are in every case smaller than the point sizes. The values of the different quantities at the crossing as well as the critical exponents are shown in Table II.

TABLE II. Lattice-size-dependent estimates of critical quantities for the microcanonical $D=3$ Ising model. The displayed quantities are crossing points $e_{c,L,2L}$ for the correlation length in units of the lattice size, ξ/L itself at those crossing points, and the estimates for the correlation length exponent ν_m and the anomalous dimension η. All quantities are obtained using parabolic interpolations.

L	$e_{c,L,2L}$	$\xi_{L,e_{c,L,2L}}/L$	ν_m	η_m
8	−0.861831(12)	0.44922(3)	0.8033(42)	0.0564(2)
12	−0.865010(10)	0.46106(5)	0.7968(31)	0.0492(4)
16	−0.866020(6)	0.46710(5)	0.7717(22)	0.0469(4)
24	−0.866767(3)	0.47411(4)	0.7665(11)	0.0437(3)
32	−0.867034(4)	0.47813(6)	0.7594(13)	0.0425(5)
48	−0.867228(2)	0.48278(5)	0.7492(5)	0.0412(3)
64	−0.867302(2)	0.48555(11)	0.7457(16)	0.0397(8)

The numerical estimates for e_c, $\xi_{L,e_c}/L$ and the critical exponents ν_m and η obtained using the quotients method for pair of lattices $(L,2L)$ are quoted in Table II. Our small statistical errors allow to detect a tiny L evolution. An extrapolation to infinite volume is clearly needed.

Before going on, let us recall our expectations as obtained applying Fisher renormalization to the most accurate determination of *canonical* critical exponents known to us [$\nu_m = \nu/(1-\alpha) = \nu/(D\nu-1)$],

$$\nu_m = 0.7077(5) (\text{from } \nu = 0.6301(4) \quad [33]), \tag{45}$$

$$\eta_m = \eta = 0.036\,39(15) \quad [34], \tag{46}$$

$$\omega = 0.84(4) \quad [33]. \tag{47}$$

Besides, although nonuniversal, let us quote $e_c = -0.867\,433(12)$ [39].

The results obtained from an extrapolation using only leading-order scaling corrections were:

$$\text{(i)} \quad e_c = -0.867\,397(6), \quad \omega + 1/\nu_m = 1.918(26)$$

(we obtained a good fit for $L \geq L_{\min} = 12$, with $\chi^2/\text{NDF} = 0.39/3$, CL=94%, where "NDF" stands for *number of degrees of freedom* and "CL" for *confidence level* [40]).

$$\text{(ii)} \quad \xi_{e_c,L}/L = 0.5003(12), \quad \omega = 0.581(27),$$

($L_{\min} = 12$, $\chi^2/\text{NDF} = 0.12/3$, CL=99%).

$$\text{(iii)} \quad \nu_m = 0.714(28), \quad \omega = 0.53(30),$$

($L_{\min} = 8$, $\chi^2/\text{NDF} = 3.16/4$, CL=53%).

$$\text{(iv)} \quad \eta = 0.0391(15), \quad \omega = 1.21(24),$$

($L_{\min} = 8$, $\chi^2/\text{NDF} = 0.96/4$, CL=92%). The main conclusions that we draw from these fits are: (i) the exponents are compatible with our expectations from Fisher renormalization, (ii) subleading scaling corrections are important given the tendency of the fits to produce a too low estimate for ω (see below), and (iii) the estimates from canonical exponents (obtained themselves by applying the high-temperature expansion to improved Hamiltonians [41,42]) are more accu-

rate than our direct computation in the microcanonical ensemble.

We can, instead, take an opposite point of view. If we take the central values in Eqs. (45)–(47), as if they were exact, we can obtain quite detailed information on the amplitudes for scaling corrections:

(i) We find an excellent fit to $\nu_m(L,2L)=\nu_m+A_1L^{-\omega}+A_2L^{-2\omega}$, for $L_{\min}=16:\chi^2/\mathrm{NDF}=1.53/3$, CL=68%, with $A_1=1.38(7)$ and $A_2=-7.6(1.1)$. This confirms our suspected strong subleading corrections. Indeed, according to these amplitudes A_1 and A_2, only for $L\approx 130$ the contribution of the (subleading) quadratic term becomes a 10% of that of the leading one.

(ii) In the case of $\eta(L,2L)=\eta+B_1L^{-\omega}+B_2L^{-2\omega}$, for $L_{\min}=8:\chi^2/\mathrm{NDF}=2.4/5$, CL=79%, we have $B_1=0.101(10)$ and $B_2=0.07(7)$. Subleading scaling corrections are so small that, within our errors, it is not clear whether $B_2=0$ or not.

The quite strong scaling corrections found for ν_m may cast some doubts in the extrapolation for $\xi_{L,e_c}/L$, the only quantity that we cannot double check with a canonical computation. To control this, we proceed to a fit including terms linear and quadratic in $L^{-\omega}$ with $\omega=0.84(4)$. We get

$$\frac{\xi_{L,e_c}}{L}=0.4952(5)(7),$$

with $L_{\min}=12$, $\chi^2/3=2.17/3$, and CL=54%. Here, the second error is due to the quite small uncertainty in ω. It is remarkable that the contribution to the error stemming from the error in ω is *larger* than the purely statistical one.

Canonical specific heat

Previous numerical studies of microcanonical FSS [16–18] focused on the specific heat. Although we show all across this paper that a complete microcanonical FSS analysis can be based only on the spin propagator, the specific heat can be certainly studied within the present formalism.

As discussed in Sec. II A (see also [3]), the canonical specific heat can be estimated from the microcanonical estimator $C_m(L,e)$ defined in Eq. (22). The expected FSS behavior for $C_m(L,e_{c,L,2L})$ is

$$C_m(L,e_{c,L,2L})=L^{\alpha/\nu}[A_0+A_1L^{-\omega}+\cdots]+B. \qquad (48)$$

Here, A_0 and A_1 are scaling amplitudes, while B is a constant background usually termed *analytical correction to scaling*, stemming from the nonsingular part of the free energy [10]. It is usually disregarded as it plays the role of a subleading scaling-correction term. Yet, a peculiarity of the $D=3$ Ising model is that B is anomalously large (see, e.g., [18]) and needs to be considered.

In Fig. 3, we reproduce the analysis of Bruce and Wilding [18], where the amplitude A_1 in Eq. (48) was fixed to zero by hand. In this way, if we consider the range of lattice sizes $8\le L\le 64$ (in [18], only $L\le 32$ was considered), we obtain $B=-35.01(11)$ but with an untenable $\chi^2/\mathrm{NDF}=227/5$. Our value of B is, nevertheless, quite close to the result $B=-34.4(4)$ reported in [18] (unfortunately, these authors provided no information on fit quality).

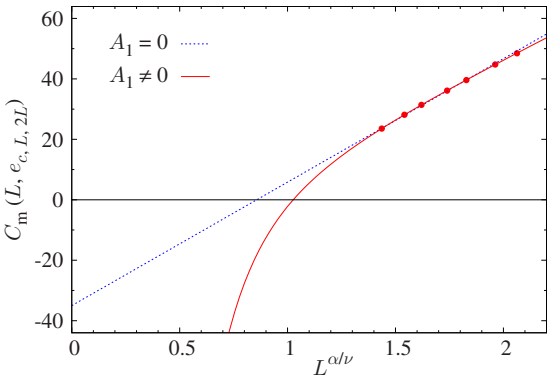

FIG. 3. (Color online) Microcanonical estimate of the specific heat, $C_m(L,e)$, at $e_{c,L,2L}$ for the $D=3$ Ising model, as a function of the system size. The numerical estimates of exponents α/ν and ω were taken from Ref. [41]. The error bars are in every case smaller than the point sizes. The solid line is a fit to Eq. (48) (fitting parameters: A_0, A_1, and B) and the dashed one is obtained by constraining the fit to $A_1=0$.

Once the arbitrary constraint $A_1=0$ is removed, we do obtain an acceptable fit, $\chi^2/\mathrm{NDF}=0.68/4$. Perhaps unsurprisingly, the estimate of B is largely changed once a nonvanishing A_1 is allowed: $B=-24.4(7)$.

VII. RESULTS FOR THE $D=2$, $Q=4$ POTTS MODEL

The $Q=4$, $D=2$ Potts model offers two peculiarities that will be explored here. First, it suffers from quite strong logarithmic scaling corrections, and second, it displays pseudometastability [33], an ideal playground for a microcanonical study.

The model has been analytically studied in the past in the canonical ensemble [26–30]. In particular, the analysis of the renormalization-group (RG) equations reveals the presence of multiplicative scaling corrections [27]. Such corrections appear as well in the FSS behavior [28–30]. This is one of the possible forms that scaling corrections can take in the limit $\omega\to 0$ and is a great nuisance for numerical studies. A very detailed theoretical input, such as the one in Ref. [30], is mandatory to perform safely the data analysis. We shall make here an educated guess for the *microcanonical* form of the scaling corrections, based purely in ensemble equivalence and in the *canonical* results.

From ensemble equivalence, we expect

$$e-e_c\sim C(L,\beta_c)\Delta\beta_L, \qquad (49)$$

where $C(L,\beta_c)$ is the finite-lattice canonical specific heat at β_c and $\Delta\beta=\beta_c^{(L)}-\beta_c$ is the inverse-temperature distance to the critical point of any L-dependent feature (such as the temperature maximum of the specific heat, etc.). We borrow from Ref. [30] the leading FSS behavior for these quantities

$$C(L,\beta_c)\sim\frac{L}{(\log L)^{3/2}},\quad \Delta\beta_L\sim\frac{(\log L)^{3/4}}{L^{3/2}}. \qquad (50)$$

Thus, we have

$$e(L) - e_c(\infty) \sim L^{-1/2}(\log L)^{-3/4}. \tag{51}$$

This result can be derived as well by considering only the leading terms of the first derivative of the singular part of free energy with respect to the thermal field, ϕ ($\propto \beta - \beta_c$) [30]

$$\frac{\partial f_{\text{sing}}(\phi,h,\psi)}{\partial \phi} \approx \frac{4}{3} D_{\pm} |\phi|^{1/3} (-\log|\phi|)^{-1} + D_{\pm} |\phi|^{4/3} (-\log|\phi|)^{-2} \frac{1}{\phi}. \tag{52}$$

The previous equation describes the energy of the system and its leading term is

$$e - e_c \sim \frac{4}{3} D_{\pm} \frac{|\phi|^{1/3}}{\log|\phi|}, \tag{53}$$

but

$$\phi \approx C'_{\pm} L^{-3/2} (\log L)^{3/4}, \tag{54}$$

so it is direct to obtain again Eq. (51). Hence, we are compelled to rephrase Eq. (28) as

$$\langle O \rangle_{L,e} = L^{x_{O,m}/\nu_m} \tilde{f}_O [L^{1/2} (\log L)^{3/4} (e - e_c)] + \cdots. \tag{55}$$

Furthermore, from the canonical analysis [30], we expect multiplicative logarithmic corrections to the susceptibility (that do not get Fisher-renormalized). Furthermore, the dots in Eq. (55) stand for corrections of order $\log\log L/\log L$ and $1/\log L$ [30].

We first address in Sec. VII A the direct verification of Eq. (55) using the quotients method. We consider afterwards the pseudometastability features.

A. Scaling plots and critical exponents

We start by a graphical demonstration of Eq. (55). ξ/L as a function of $(e-e_c)L^{1/2}(\log L)^{3/4}$ should collapse onto a single curve (the deviation will be bigger for small L values due to neglected scaling corrections of order $\log\log L/\log L$ and $1/\log L$) [43]. A similar behavior is expected for the scaled susceptibility [30]

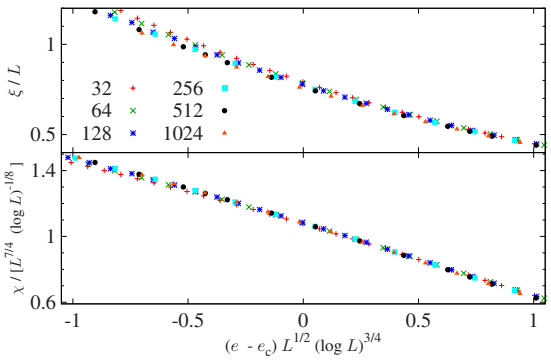

FIG. 4. (Color online) Graphical demonstration of Eq. (55) as applied to the microcanonical $D=2$, $Q=4$ Potts model. Both the correlation length in units of the lattice size (top) and the scaled susceptibility, $\bar{\chi}$ in Eq. (56) (bottom), are functions of the scaling variable $(e-e_c)L^{1/2}(\log L)^{3/4}$.

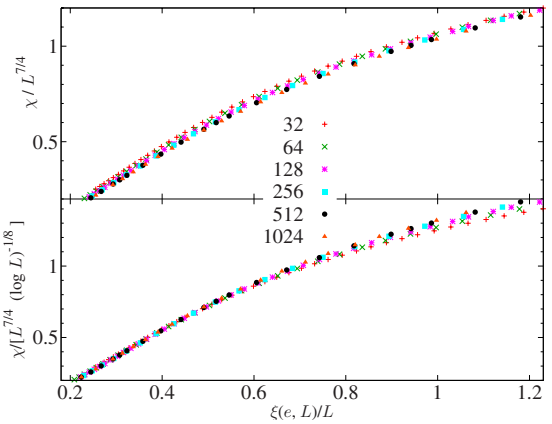

FIG. 5. (Color online) Comparison of the scaling for the naively scaled susceptibility $\chi L^{-7/4}$ (top) and for $\bar{\chi}$ (bottom) as a function of the correlation length in units of the lattice size, for the microcanonical $D=2$, $Q=4$ Potts model.

$$\bar{\chi} = \frac{\chi}{L^{7/4} (\log L)^{-1/8}}. \tag{56}$$

Note that ξ/L does not need an additional logarithmic factor. These expectations are confirmed in Fig. 4, especially for the largest system sizes (that suffer lesser scaling corrections).

We can check directly the importance of the multiplicative logarithmic corrections for the susceptibility by comparing χ and $\bar{\chi}$ as a function of ξ/L (Fig. 5). The improved scaling of $\bar{\chi}$ is apparent. We observe as well that the largest corrections to scaling are found at and below the critical point (around $\xi/L \approx 1.0$).

The scaling proposed for the susceptibility in Ref. [30] can also be checked from our values at $e_{c,L,2L}$. Considering $\chi \sim L^{7/4}$ (our data is fully supportive of this point), we can plot $\log(\chi/L^{7/4})$ versus $\log\log L$ to obtain a linear fit for the data with $L>64$ with a slope $-0.132(3)$ ($\chi^2/\text{NDF}=7.5/1$) (see the dashed line in Fig. 6, which can be compared to the expected value $-1/8$ [30]). The high value of χ^2/NDF can be ascribed to the presence of higher-order correction terms.

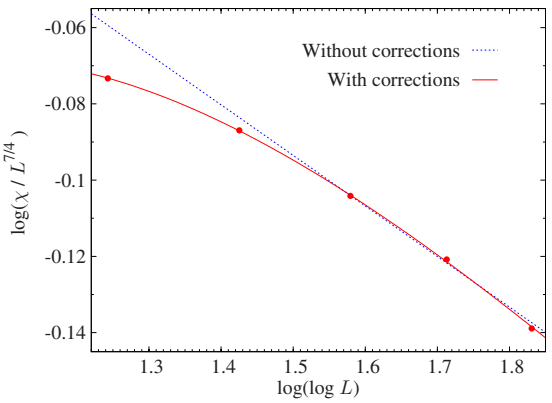

FIG. 6. (Color online) Logarithmic scaling behavior of the susceptibility at the critical point. The error bars are in every case smaller than the point sizes. Dashed line does not include the subleading additive terms of Eq. (57) while the solid line does.

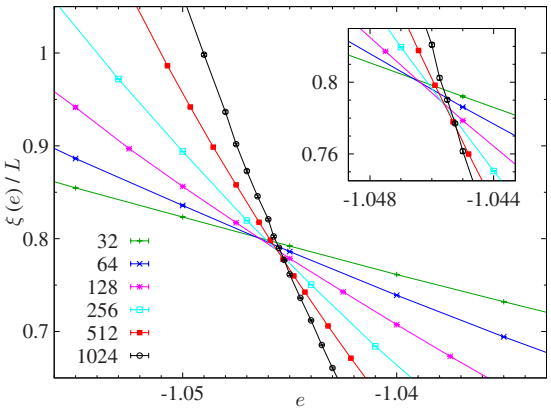

FIG. 7. (Color online) Correlation length in lattice size units for the two-dimensional $Q=4$ Potts model. The values of the different quantities on the crossings for lattices L and $2L$, as well as the corresponding estimate for critical exponents, are in Table III. The inset is a magnification of the critical region.

In fact, the whole scaling behavior for the susceptibility is [30]

$$\chi \sim L^{7/4}(\log L)^{-1/8}\left(1 + A\frac{\log\log L}{\log L} + B\frac{1}{\log L} + \cdots\right) \tag{57}$$

and we can use this form for a least-squares fit. Fixing both the leading and the logarithmic exponents, we estimate $A=0.80(7)$ and $B=-0.48(3)$ using all the lattice sizes with $\chi^2/\mathrm{NDF}=2.9/2$ (see the solid line in Fig. 6). Therefore, our data set is fully supportive of the behavior proposed in Ref. [30], including the subleading additive logarithmic corrections.

We now proceed to the numerical computation of critical exponents. We shall use the quotients method, modified as described in the Appendix. As it is evident from Fig. 7, the crossing points can be obtained with great accuracy using parabolic interpolations of the nine points around the estimated crossing energies (see Sec. IV). We checked that the results do not depend on the interpolating polynomial degree by comparing to interpolations using cubic curves. We also compared to the results obtained using only seven points around the crossing obtaining again full agreement.

The obtained critical exponents are shown in Table III. We may compare them to the exact ones [36] ($\nu=2/3$, $\alpha=2/3$, and $\eta=1/4$)

$$\nu_m = 2; \quad \eta = \eta_m = \frac{1}{4}. \tag{58}$$

Comparing to our computed exponents, we obtain an acceptable agreement. In the case of the microcanonical ν exponent, ν_m, after adding the correction for the quotients method in presence of logarithms, the agreement is fairly good. We can see a clear trend towards the exact result value for all the lattice sizes except for the biggest one (2.5 standard deviations away), which is probably due to a bad estimation of the huge temperature derivatives of the correlation length. In the case of the microcanonical η exponent, η_m, which must be the same that the canonical one, we can see clearly the tendency to the analytical value $\eta_m=0.25$. We must remark the importance of adding the corrections described in the Appendix to the quotients method.

B. Critical point, latent heat, and surface tension

It has been known for quite a long time that the $D=2$, $Q=4$ Potts model on finite lattices show features typical of first-order phase transitions [33]. For instance (see Fig. 8), the probability distribution function for the internal energy, $P_\beta(e)$, displays two peaks at energies e_d (the coexisting *disordered* phase) and e_o (the energy of the *ordered* phase) separated by a minimum at e^*. Of course, since the transition is of the second order, e_c is the common large L limit of e_d, e_o, and e^*.

We discussed in Sec. II B how the Maxwell's construction is used to estimate the canonical critical point $\beta_{c,L}$, as well as e_d, e_o, and the associated surface tension. This procedure is outlined in Fig. 9. The numerical results are in Table IV, where we see that $\beta_{c,L}$ is a monotonically increasing function of L continuously approaching to the analytical value $\beta_c=\log(1+\sqrt{Q})=1.098\,612\,2\ldots$ [44]. A jackknife method [10] is used to compute the error bars for all quantities in Table IV.

To perform a first check of our data, we observe that $\beta_{c,L}$ is a typical *canonical* estimator of the inverse critical temperature. As such, it is subject to standard canonical FSS, where the main scaling corrections come from two additive logarithmic terms [30]

TABLE III. Crossing points of the correlation length in lattice size units as a function of the energy for pairs of lattices $(L,2L)$. Using the original quotients method [10], we obtain the microcanonical critical exponents, shown in the columns 4 and 6, while the corrected ones (columns 5 and 7) are labeled with primed symbols (see the Appendix).

L	$e_{c,L,2L}$	$\xi_{L,e_{c,L,2L}}/L$	ν_m	ν'_m	η_m	η'_m
32	−1.04659(5)	0.8016(5)	1.534(6)	1.998(10)	0.2663(9)	0.2334(9)
64	−1.04633(2)	0.7990(3)	1.554(8)	1.957(12)	0.2638(6)	0.2360(6)
128	−1.04579(1)	0.7909(3)	1.578(5)	1.938(7)	0.2639(5)	0.2398(5)
256	−1.04548(2)	0.7836(5)	1.643(12)	1.987(17)	0.2615(11)	0.2402(11)
512	−1.04519(2)	0.7734(9)	1.602(31)	1.895(42)	0.2617(21)	0.2427(21)

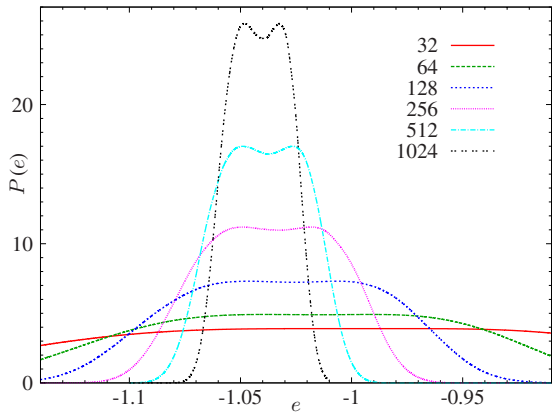

FIG. 8. (Color online) *Canonical* probability distribution function for the energy density, $P_\beta^{(L)}(e)$, as reconstructed from microcanonical simulations of the $D=2$, $Q=4$ Potts model and different system sizes. The L-dependent critical point $\beta_{c,L}$ is computed using the Maxwell's rule, Sec. II B (note the equal height of the two peaks enforced by Maxwell's construction). The system displays an apparent latent heat that becomes smaller for growing L and vanishes in the large L limit.

$$\beta_{c,L} - \beta_c = a_1 \frac{(\log L)^{3/4}}{L^{3/2}} \left(1 + a_2 \frac{\log\log L}{\log L} + a_3 \frac{1}{\log L} \right). \tag{59}$$

From our data in Table IV, we obtain $a_1=-0.44(7)$, $a_2=-1.15(72)$, and $a_3=2.28(26)$ and a good fit ($L_{\min}=128:\chi^2/\mathrm{NDF}=0.28/1$, CL=60%).

As for the L dependence of e_d and e_o, we try a fit that consider the expected scaling-correction terms [30]

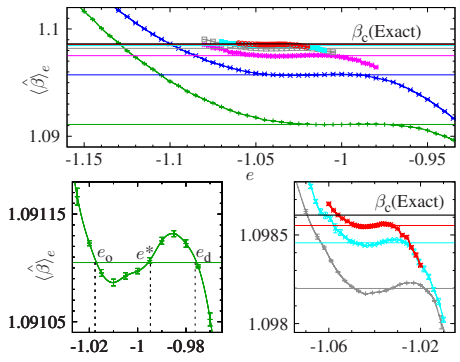

FIG. 9. (Color online) (Top) From the microcanonical mean values $\langle\hat{\beta}\rangle_{e,L}$ for the $D=2$, $Q=4$ Potts model, we estimate the size-dependent *canonical* inverse critical temperature $\beta_{c,L}$ (horizontal lines) for all the simulated lattice sizes, ranging from $L=32$ (lower) to $L=1024$ (upper). We show as well the analytical prediction (upper horizontal line). (Bottom left) Example of Maxwell's construction for our $L=32$ data. The e integral of $\langle\hat{\beta}\rangle_{e,L}-\beta_{c,L}$ from e_o to e_d vanishes. (Bottom right) Zoom of upper panel showing only data for lattice sizes $L=256$ (lower curve), $L=512$ (medium curve), and $L=1024$ (upper curve).

TABLE IV. Using Maxwell's construction, we compute for the $D=2$, $Q=4$ Potts model the L-dependent estimate of the (inverse) critical temperature $\beta_{c,L}$, the energies of the coexisting ordered phase e_o, and disordered phase e_d, as well as the surface tension (Σ).

L	$\beta_{c,L}$	e_o	e_d	$\Sigma\times 10^5$
32	1.0911070(20)	−1.0175(4)	−0.9760(2)	0.47(2)
64	1.0957256(14)	−1.0392(3)	−0.9915(2)	2.77(7)
128	1.0975150(10)	−1.0463(3)	−1.0062(5)	4.10(15)
256	1.0981989(5)	−1.0489(2)	−1.0183(3)	3.92(8)
512	1.0984570(3)	−1.0490(1)	−1.0266(2)	3.28(11)
1024	1.0985539(3)	−1.0483(3)	−1.0325(1)	2.09(17)

$$e_{c,o,L} - e_c = a_1 L^{-1/2} (\log L)^{-3/4} \left(1 + a_2 \frac{\log\log L}{\log L} + a_3 \frac{1}{\log L} \right). \tag{60}$$

Our results for e_o are $a_{1o}=-2.03(20)$, $a_{2o}=-1.65(27)$, and $a_{3o}=-2.08(41)$, with a fair fit quality ($L_{\min}=32:\chi^2/\mathrm{NDF}=2/3$, CL=57%). On the other hand, we obtain for e_d:$a_{1d}=2.02(14)$, $a_{2d}=0.93(37)$, and $a_{3d}=-2.93(34)$, with a fair fit as well ($L_{\min}=32:\chi^2/\mathrm{NDF}=0.84/3$, CL=84%). These two fits are shown in Fig. 10.

For the surface tension, we note in Table IV a nonmonotonic behavior. Furthermore, we lack a theoretical input allowing us to fit. We thus turn to a variant of the quotients method. Where Σ to follow a pure power-law scaling, $\Sigma \propto L^b$, exponent b would be obtained as

$$\frac{\Sigma(L_1)}{\Sigma(L_2)} = \left(\frac{L_1}{L_2} \right)^b \Rightarrow b = \frac{\log[\Sigma(L_1)/\Sigma(L_2)]}{\log(L_1/L_2)}. \tag{61}$$

The effective exponent b obtained from our data is displayed in Table V. We observe that it is clearly negative (as it should since Σ vanishes for a second-order phase transition). An

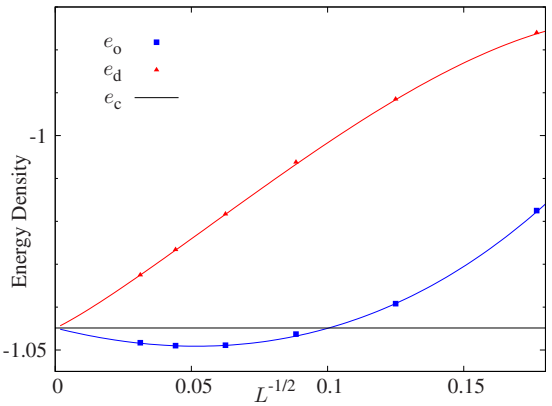

FIG. 10. (Color online) System-size-dependent estimates for the energies of the "coexisting" ordered (e_o, blue squares) and disordered (e_d, red triangles) phases of the $D=2$, $Q=4$ Potts model as a function of $L^{-1/2}$. Lines are fits to the expected analytical behavior Eq. (60). Horizontal line corresponds to the asymptotic value, e_c.

TABLE V. Effective exponent obtained using Eq. (61) for the surface tension.

(L_1, L_2)	$b_{\rm eff}(\Sigma)$
(32,64)	2.56(7)
(64,128)	0.56(6)
(128,256)	–0.065(60)
(256,512)	–0.257(57)
(512,1024)	–0.650(127)

asymptotic estimate, however, seems to require the simulation of larger systems.

We have just seen that, up to scaling corrections, $e_d^{(L)}$ and $e_o^{(L)}$ correspond to (different) L-independent values of the argument of the scaling function $\tilde{f}_\xi$ in Eq. (55). Hence, we expect that $\xi(e_d)/L$ and $\xi(e_o)/L$ (see Table VI) approach nonvanishing, different values in the large L limit. The finite-size scaling corrections are expected to be additive logarithms [30]

$$\frac{\xi}{L} = a + \frac{b}{\log L}. \tag{62}$$

The results are

$$\frac{\xi(e_o)}{L} = 1.28(1) - \frac{2.28(5)}{\log L} \tag{63}$$

($L_{\rm min}=32: \chi^2/{\rm NDF}=4.2/3$, CL=22%) and

$$\frac{\xi(e_d)}{L} = 0.159(4) - \frac{0.98(2)}{\log L} \tag{64}$$

($L_{\rm min}=32: \chi^2/{\rm NDF}=3.3/3$, CL=37%).

A very similar analysis can be performed for the scaled susceptibility, Eq. (43), at e_d and e_o. In order to deal with the multiplicative logarithms of the susceptibility, we rather used $\bar{\chi}$ defined in Eq. (56).

Fitting our data set to the logarithmic form

$$\bar{\chi} = A + B\frac{\log\log L}{\log L}, \tag{65}$$

obtained in Ref. [30], we obtain a good fit in the ordered-phase energy, e_o,

$$\bar{\chi}(e_o) = 2.41(5) - 4.00(15)\frac{\log\log L}{\log L}, \tag{66}$$

($L_{\rm min}=128: \chi^2/{\rm NDF}=3.10/2$, CL=21%). On the other hand, the extrapolation for the susceptibility defined in the disordered phase energy, e_d, is a nonsensical negative value.

We can also fit the data to the logarithmic form also used in Ref. [30]

$$\bar{\chi} = A + \frac{B}{\log L}, \tag{67}$$

finding

$$\bar{\chi}(e_o) = 1.643(5) - \frac{2.55(2)}{\log L} \tag{68}$$

($L_{\rm min}=32: \chi^2=7.44/4$, CL=11%) and

$$\bar{\chi}(e_d) = 0.094(7) + \frac{1.87(37)}{\log L}, \tag{69}$$

($L_{\rm min}=64: \chi^2/{\rm NDF}=2.94/3$, CL=37%). For comparison, we recall that Ref. [30] reports two different fits for $\bar{\chi}$, depending of the logarithmic corrections they used

$$\bar{\chi}^{\rm canonical} = 1.673(33) - 1.056(98)\frac{\log\log L}{\log L}, \tag{70}$$

$$\bar{\chi}^{\rm canonical} = 1.454(13) - \frac{0.600(55)}{\log L}. \tag{71}$$

VIII. CONCLUSIONS

We have formulated the FSSA for microcanonical systems in terms of quantities accessible in a finite lattice. This form allows extending the phenomenological renormalization approach (the so-called quotients method) to the microcanonical framework.

TABLE VI. Correlation length in units of the lattice size and the RG invariant $\bar{\chi}$ defined in Eq. (56), for several L values, as computed in the microcanonical $D=2$, $Q=4$ Potts model. The chosen values of the energy density correspond to the ordered (e_o) and disordered (e_d) phases. For comparison, we also display the *canonical* results at β_c obtained in Ref. [30].

L	$\xi(e_o)/L$	$\xi(e_d)/L$	$\bar{\chi}(e_o)$	$\bar{\chi}(e_d)$	$\xi^{\rm canonical}/L$	$\bar{\chi}^{\rm canonical}$
32	0.637(2)	0.453(1)	0.990(3)	0.907(2)	0.647(1)	1.287(3)
64	0.732(3)	0.396(1)	0.995(2)	1.025(3)	0.545(2)	1.310(2)
128	0.799(5)	0.357(4)	1.001(3)	1.106(5)	0.472(7)	1.331(3)
256	0.866(6)	0.335(3)	1.001(5)	1.182(6)	0.429(5)	1.343(5)
512	0.915(4)	0.315(2)	1.014(8)	1.238(4)	0.392(4)	1.366(8)
1024	0.953(15)	0.302(2)	0.997(21)	1.279(13)	0.367(3)	1.353(22)

Our FSSA has been subjected to a quite strong numerical testing. We have performed extensive microcanonical numerical simulations in two archetypical systems in statistical mechanics: the three-dimensional Ising model and the two-dimensional four-state Potts model. The two models present a power-law singularity in their canonical specific heat, implying nontrivial Fisher renormalization when going to the microcanonical ensemble. A microcanonical cluster method works for both models, hence allowing us study very large system sizes ($L=128$ in $D=3$ and $L=1024$ in $D=2$).

In the case of the Ising model, we have obtained precise determinations of the critical exponents that, we feel, provide strong evidence for our extended microcanonical FSSA. For the Potts model, strong logarithmic corrections (both multiplicative and additive) plague our data. Fortunately, we have a relatively good command on these corrections from canonical studies [30]. Our data can be fully rationalized using the scaling corrections suggested by the theoretical analysis [30].

ACKNOWLEDGMENTS

We have been partly supported through Research Contracts No. FIS2006-08533-C03, No. FIS2007-60977 (MICINN, Spain), and No. GR58/08, 910383 (Banco de Santander-UCM). The simulations for this work were performed at BIFI.

APPENDIX: THE QUOTIENTS METHOD IN THE PRESENCE OF MULTIPLICATIVE LOGARITHMIC CORRECTIONS

The quotients method [10,25] has been widely used in the past for the computation of critical exponents. Yet, its convergence to the large L limit is extremely slow in presence of multiplicative logarithmic scaling corrections. Fortunately, let us show how we can speed up convergence if we have enough analytical information at our disposal.

Let us consider an observable O such that its FSS behavior is given by (z can be either the reduced temperature t or $e-e_c$)

$$O(L,z) = L^{x_O/\nu}(\log L)^{\hat{x}_O}\left[F_O\left(\frac{L}{\xi(L,z)}\right) + \cdots \right], \quad \text{(A1)}$$

then the critical exponent calculated using Eq. (32) must be corrected following

$$\frac{x'_O}{\nu} = \frac{x_O}{\nu} - \frac{\hat{x}_O}{\log(L_2/L_1)}\log\left(\frac{\log L_2}{\log L_1}\right). \quad \text{(A2)}$$

Specifically for the two-dimensional four-state Potts model, the values of the logarithmic correction exponents are analytically known [27–30], thus we can compute accurately the corrections in this case. In addition, the susceptibility behaves as

$$\chi \sim L^{7/4}(\log L)^{-1/8}, \quad \text{(A3)}$$

so we easily get

$$\eta' = \eta - \frac{1}{8\log(L_2/L_1)}\log\left(\frac{\log L_2}{\log L_1}\right). \quad \text{(A4)}$$

For the correlation length, it is known that

$$\xi \sim |t|^{-2/3}(-\log t)^{1/2}; \quad t \sim L^{-3/2}(\log L)^{3/4} \quad \text{(A5)}$$

and therefore the temperature derivative scales as

$$\partial_\beta \xi \sim L^{5/2}(\log L)^{-3/4}, \quad \text{(A6)}$$

resulting in a ν canonical exponent correction of

$$\nu' = \nu\left[1 - \frac{3}{4}\frac{\nu}{\log(L_2/L_1)}\log\left(\frac{\log L_2}{\log L_1}\right)\right], \quad \text{(A7)}$$

while for the microcanonical ν exponent, ν_m, we use that

$$e \sim L^{-1/2}(\log L)^{-3/4} \quad \text{(A8)}$$

and

$$\partial_e \xi \sim L^{3/2}(\log L)^{3/4}. \quad \text{(A9)}$$

Hence,

$$\nu'_m = \nu_m\left[1 + \frac{3}{4}\frac{\nu_m}{\log(L_2/L_1)}\log\left(\frac{\log L_2}{\log L_1}\right)\right]. \quad \text{(A10)}$$

[1] Depending on context, sometimes the grand-canonical and canonical ensembles are on the same relative position than the canonical and microcanonical ones.
[2] W. Janke, Nucl. Phys. B (Proc. Suppl.) **63**, 631 (1998); Similar ideas, although less explicit in their use of a microcanonical language, were developed in M. S. S. Challa, D. P. Landau, and K. Binder, Phys. Rev. B **34**, 1841 (1986); J. Lee and J. M. Kosterlitz, Phys. Rev. Lett. **65**, 137 (1990).
[3] V. Martin-Mayor, Phys. Rev. Lett. **98**, 137207 (2007).
[4] L. A. Fernandez, A. Gordillo-Guerrero, V. Martin-Mayor, and J. J. Ruiz-Lorenzo, Phys. Rev. Lett. **100**, 057201 (2008).
[5] D. H. E. Gross, *Microcanonical Thermodynamics: Phase Transitions in "Small" Systems*, Lectures Notes in Physics Vol. 66 (World Scientific, Singapore, 2001).
[6] R. Lustig, J. Chem. Phys. **109**, 8816 (1998).
[7] K. Binder, Z. Phys. B **43**, 119 (1981).
[8] M. N. Barber, in *Phase Transitions and Critical Phenomena 8*, edited by C. Domb and J. L. Lebowitz (Academic Press, New York, 1983).
[9] *Finite Size Scaling and Numerical Simulations of Statistical Systems*, edited by V. Privman (World Scientific, Singapore, 1990).
[10] D. Amit and V. Martin-Mayor, *Field Theory, the Renormalization Group and Critical Phenomena*, 3rd ed. (World Scientific, Singapore, 2005).
[11] M. E. Fisher, Phys. Rev. **176**, 257 (1968).
[12] V. Dohm, J. Phys. C **7**, L174 (1974).
[13] We follow the standard terminology (see, e.g., [10]) for the

critical exponents: ν is the exponent for the correlation length, α that of the specific heat, β that of the order parameter, while ω is the (universal) leading-order scaling-corrections exponent. A slightly different exponent, the anomalous dimension, is defined in Eq. (26).

[14] In the particular case of the fixed-energy constraint, Eq. (2) follows from Eq. (1) and from the ensemble equivalence property $\langle O\rangle_{L=\infty,e}=\langle O\rangle_{L=\infty,T}^{\text{canonical}}$, if $e=\langle e\rangle_{L=\infty,T}^{\text{canonical}}$. Indeed, it suffices to notice that [$C(T)$ is the canonical specific heat, $C \propto |t|^{-\alpha}$], $e-e_c=\int_{T_c}^{T} dTC(T) \propto |t|^{1-\alpha} \to |t| \propto |e-e_c|^{1/1-\alpha}$. The only exponent whose renormalization is not clear at this point is α itself, for the energy is not a dynamical variable but a parameter in this ensemble. If one chooses to define α_m as the critical exponent corresponding to dt/de, the correspondence with Fisher renormalization, $\alpha_m=-\alpha/(1-\alpha)$ becomes complete. In fact, see concluding paragraph in Sec. II A, the microcanonical dt/de behaves as the canonical $1/[de/dt]$. Note that in the above expressions, we disregarded subdominant terms such as the contribution of the analytical background in the specific heat. Such terms are subdominant only if $\alpha>0$. In case α were negative, the asymptotic dominance is different. The specific heat at T_c is dominated by the analytical background. As a consequence, $|t| \sim |e-e_c|$ and none of the exponents (not even α) gets renormalized.

[15] R. Kenna, H.-P. Hsu, and C. von Ferber, J. Stat. Mech.: Theory Exp. **2008**, L10002 (2008).

[16] R. C. Desai, D. W. Heermann, and K. Binder, J. Stat. Phys. **53**, 795 (1988).

[17] M. Kastner, M. Promberger, and A. Hüller, J. Stat. Phys. **99**, 1251 (2000).

[18] A. D. Bruce and N. B. Wilding, Phys. Rev. E **60**, 3748 (1999).

[19] M. Kastner and M. Promberger, J. Stat. Phys. **103**, 893 (2001).

[20] H. Behringer and M. Pleimling, Phys. Rev. E **74**, 011108 (2006).

[21] A. Tröster, Phys. Rev. Lett. **100**, 140602 (2008).

[22] S. Caracciolo, R. G. Edwards, S. J. Ferreira, A. Pelissetto, and A. D. Sokal, Phys. Rev. Lett. **74**, 2969 (1995).

[23] F. Cooper, B. Freedman, and D. Preston, Nucl. Phys. B **210**, 210 (1982).

[24] M. P. Nightingale, Physica A **83**, 561 (1975).

[25] H. G. Ballesteros, L. A. Fernandez, V. Martin-Mayor, and A. Muñoz Sudupe, Phys. Lett. B **378**, 207 (1996); **387**, 125 (1996); Nucl. Phys. B **483**, 707 (1997).

[26] M. P. M. den Nijs, J. Phys. A **12**, 1857 (1979); B. Nienhuis, E. K. Riedel, and M. Schick, *ibid.* **13**, L189 (1980).

[27] M. Nauenberg and D. J. Scalapino, Phys. Rev. Lett. **44**, 837 (1980); J. L. Cardy, M. Nauenberg, and D. J. Scalapino, Phys. Rev. B **22**, 2560 (1980).

[28] J. L. Black and V. J. Emery, Phys. Rev. B **23**, 429 (1981).

[29] R. Kenna, D. A. Johnston, W. Janke, Phys. Rev. Lett. **96**, 115701 (2006); **97**, 155702 (2006).

[30] J. Salas and A. D. Sokal, J. Stat. Phys. **88**, 567 (1997).

[31] S. Duane, A. D. Kennedy, B. J. Pendleton, and D. Roweth, Phys. Lett. B **195**, 216 (1987).

[32] Note that this microcanonical ensemble exactly matches the conditions in the original Fisher work [11]: the momenta are some *hidden* degrees of freedom in thermal equilibrium with the spins and a global constraint is imposed. It is also amusing to rederive the results in Sec. II considering Γ momenta per spin (in this work $\Gamma=1$, while Lustig [6] always considered $\Gamma=3$). If one takes the limit $\Gamma \to \infty$, at fixed N, the canonical probability is recovered for the spins.

[33] M. Fukugita, H. Mino, M. Okawa, and A. Ukawa, J. Phys. A **23**, L561 (1990).

[34] Note that the microcanonical weight (9) is *not* analytical at each energy level of the spin Hamiltonian.

[35] Note that, Eq. (28) tells us that, if the energy histogram is double-peaked (see Sec. II B), the histogram maxima will tend to e_c only as L^{-1/ν_m}.

[36] F. Wu, Rev. Mod. Phys. **54**, 235 (1982).

[37] M. Hasenbusch and K. Pinn, J. Phys. A **31**, 6157 (1998).

[38] H. G. Ballesteros, L. A. Fernandez, V. Martin-Mayor, A. Muñoz Sudupe, G. Parisi, and J. J. Ruiz-Lorenzo, J. Phys. A **32**, 1 (1999).

[39] For the three-dimensional Ising model at criticality, $u_c^{\text{Ising}}=-0.990\,627(24)$ [37] and $\beta_c^{\text{Ising}}=0.221\,654\,6(2)$ [38], we obtain for our Potts representation of the Ising model $e_c=(u_c^{\text{Ising}}-D)/2+1/(4\beta_c^{\text{Ising}})$.

[40] The confidence level is the probability that χ^2 would be bigger than the observed value, supposing that the statistical model is correct. As a rule, we consider a fit not good-enough whenever CL$<10\%$.

[41] A. Pelissetto and E. Vicari, Phys. Rep. **368**, 549 (2002).

[42] M. Campostrini, A. Pelissetto, P. Rossi, and E. Vicari, Phys. Rev. E **65**, 066127 (2002).

[43] We obtain the exact e_c in the thermodynamic limit from $\beta_c=\log(1+\sqrt{Q})$ [44] and $u_c=-(1+Q^{-1/2})$ [36] by applying $e_c=u_c+1/(2\beta_c)$.

[44] R. J. Baxter, J. Phys. C **6**, L445 (1973).